



Article

Oncogenic Effect of the Novel Fusion Gene *VAPA-Rab31* in Lung Adenocarcinoma

Daseul Yoon ^{1,†}, Kieun Bae ^{1,†}, Jin-Hee Kim ², Yang-Kyu Choi ¹ and Kyong-Ah Yoon ^{1,*} 

¹ College of Veterinary Medicine, Konkuk University, Seoul 05029, Korea; yds3123@naver.com (D.Y.); bkieun@naver.com (K.B.); yangkyuc@konkuk.ac.kr (Y.-K.C.)

² College of Health Science, Cheongju University, Cheongju 28503, Korea; jinheekim@cju.ac.kr

* Correspondence: kayoon@konkuk.ac.kr; Tel.: +82-2-450-3789

† These authors are equally contributed to this work.

Received: 25 April 2019; Accepted: 8 May 2019; Published: 10 May 2019



Abstract: Fusion genes have been identified as oncogenes in several solid tumors including lung, colorectal, and stomach cancers. Here, we characterized the fusion gene, *VAPA-Rab31*, discovered from RNA-sequencing data of a patient with lung adenocarcinoma who did not harbor activating mutations in *EGFR*, *KRAS* and *ALK*. This fusion gene encodes a protein comprising the N-terminal region of vesicle-associated membrane protein (VAMP)-associated protein A (VAPA) fused to the C-terminal region of Ras-related protein 31 (Rab31). Exogenous expression of *VAPA-Rab31* in immortalized normal bronchial epithelial cells demonstrated the potential transforming effects of this fusion gene, including increased colony formation and cell proliferation in vitro. Also, enhanced tumorigenicity upon *VAPA-Rab31* was confirmed in vivo using a mouse xenograft model. Metastatic tumors were also detected in the liver and lungs of xenografted mice. Overexpression of *VAPA-Rab31* upregulated anti-apoptotic protein Bcl-2 and phosphorylated CREB both in cells and xenograft tumors. Reduced apoptosis and increased phosphorylation of CREB and Erk were observed in *VAPA-Rab31*-overexpressing cells after bortezomib treatment. Elevated Bcl-2 level via activated CREB contributed to the resistance to the bortezomib-induced apoptosis. Our data suggest the oncogenic function of the novel fusion gene *VAPA-Rab31* via upregulated Bcl-2 and activated CREB in lung cancer.

Keywords: *VAPA-Rab31*; gene fusion; tumorigenicity; lung adenocarcinoma

1. Introduction

Lung cancer is a common cancer and the leading cause of cancer death worldwide [1,2]. Lung adenocarcinoma is the predominant histologic type in non-small cell lung cancer, the majority of diagnosed lung cancers [3]. Lung adenocarcinoma can be classified according to the presence of major driver mutations in *EGFR*, *KRAS*, *ALK*, and *BRAF*, which confer clinical benefits to the subset of patients harboring them [4–6]. The fusion gene of *EML4-ALK* was discovered in lung adenocarcinoma in 2007 [7]; since then, fusion alterations of *ALK*, *RET*, and *ROS1* genes have been found in about 4–7% of patients with lung adenocarcinoma [8–10]. The fusions of these genes have been identified as novel drivers demonstrating oncogenic features. Fusion genes encoding tyrosine kinase provided enhanced sensitivity to selective inhibitors. For example, crizotinib has been demonstrated to be an effective targeted therapy in patients with lung adenocarcinoma harboring *ALK* or *ROS1* fusions [11,12]. Genetic rearrangements of *RET* or fibroblast growth factor receptors (*FGFR*) are rare, but can provide clinical benefits for the patients with these mutations. Therefore, the discovery of novel gene fusions and identification of their oncogenic features are important to elucidate novel targets. Here, we describe

the identification of a fusion gene comprising part of the coding regions of *Rab31* and *VAMP-associated protein A (VAPA)* through RNA-sequencing in patients with lung adenocarcinoma.

Rab31 (NM_006868) gene is a member of the RAS oncogene family that is located on chromosome 18 (18p11.22). *Rab31* protein localizes in the cytosol, Golgi apparatus and endosomes, where it functions, through its GTP-binding activity, as one of the key regulators of intracellular membrane trafficking, from the formation of vesicles to their fusion with membranes [13,14]. The promotive effect of *Rab31* on tumor progression has been reported in several kinds of cancers [15]. In glioblastoma, *Rab31* induced cell proliferation by activating G1/S checkpoint transition and the PI3K/Akt pathway [16]. *Rab31* was found to be overexpressed in estrogen receptor-positive breast cancer and enhanced proliferation of breast cancer cells [17]. Additionally, elevated *Rab31* expression was associated with poor prognosis in hepatocellular carcinoma through inhibition of apoptosis via the Bcl-2/Bax pathway [18]. *VAPA*, in turn, has been known to be involved in vesicle trafficking, membrane fusion, and cell motility [19].

In this study, we identified the fusion gene *VAPA-Rab31* in a patient with lung adenocarcinoma who did not harbor any known driver mutations in *EGFR*, *KRAS*, and *ALK*. Bronchial epithelial cells that overexpressed the fusion protein demonstrated enhanced proliferation and tumorigenicity. Our data suggest that the fusion gene *VAPA-Rab31* is a potential oncogene of lung cancer.

2. Results

2.1. Identification of the *VAPA-Rab31* Fusion Gene in a Patient with Lung Adenocarcinoma

A fusion transcript of *Rab31* and *VAPA* was detected from RNA-sequencing data of a Korean patient with lung adenocarcinoma. The patient did not harbor any activating mutation of *EGFR*, *KRAS*, or *ALK* genes; he was diagnosed as poorly differentiated lung adenocarcinoma stage 2B at the age of 51 and was a light smoker that used one pack per year. The chimeric *VAPA-RAB31* mRNA encoded a fusion protein of 379 amino acids including exon 1 to 6 of *VAPA* and exon 2 to 7 of *Rab31*, in frame; the junction between the two genes was confirmed by Sanger sequencing analysis (Figure 1A,B). *VAPA-Rab31* fusion was highly expressed only in the tumor of the patient, and not in the matched normal tissue as confirmed by RT-PCR (Figure 1C). An intrachromosomal fusion of *VAPA-Rab31* was also detected in a case of hepatocellular carcinoma from The Cancer Genome Atlas (TCGA) database (www.tumorfusions.org). Another fusion transcript of *Rab31* was detected in a patient with invasive breast carcinoma and was originated by the fusion form of *DLGAP1-Rab31* (Table S1). The tumorigenic effect of *VAPA-Rab31* has not been evaluated before; therefore, we decided to further analyze it.

2.2. Overexpression of *VAPA-Rab31* Increases Colony Formation and Upregulates *Bcl-2* Expression

To evaluate the effect of the fusion gene *VAPA-Rab31*, we stably overexpressed it in a human normal bronchial epithelial cell line (Beas-2B) using lentiviral vectors. As shown by the cell growth rate, the overexpression of *VAPA-Rab31* promoted the growth of Beas-2B cells (Figure 2A). Colony formation was also enhanced in *VAPA-Rab31*-overexpressing cells compared with control cells, overexpressing the empty vector ($p < 0.01$) (Figure 2B). Additionally, RT-PCR and immunoblot analyses showed that *VAPA-Rab31* overexpressing cells had higher levels of *Bcl-2* than the control cells (Figure 2C,D).

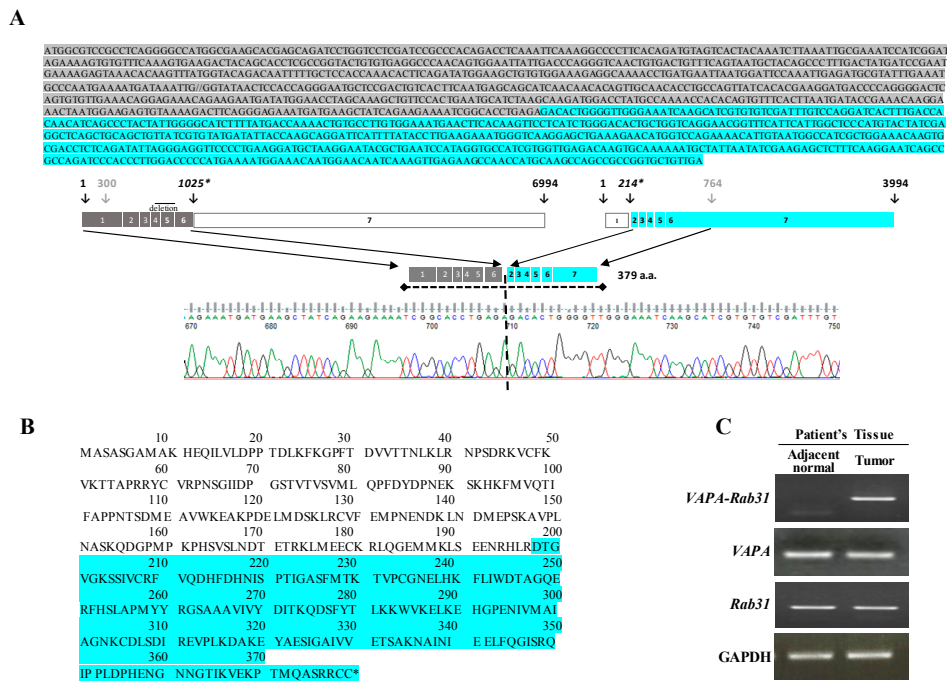


Figure 1. The VAPA-Rab31 fusion gene is highly expressed in tumor tissue of a patient with lung adenocarcinoma. (A) The VAPA and Rab31 exon structures are indicated. The schematic representation of the VAPA-Rab31 fusion gene, with the exons from each gene, is also shown. The breakpoint of the fusion gene was confirmed by Sanger sequencing chromatogram. (B) Amino acid sequences of fusion gene: different colors are used for the two gene product (grey: VAPA; blue: Rab31). (C) The overexpression of VAPA-Rab31 was confirmed by RT-PCR in the patient’s tumor tissue.

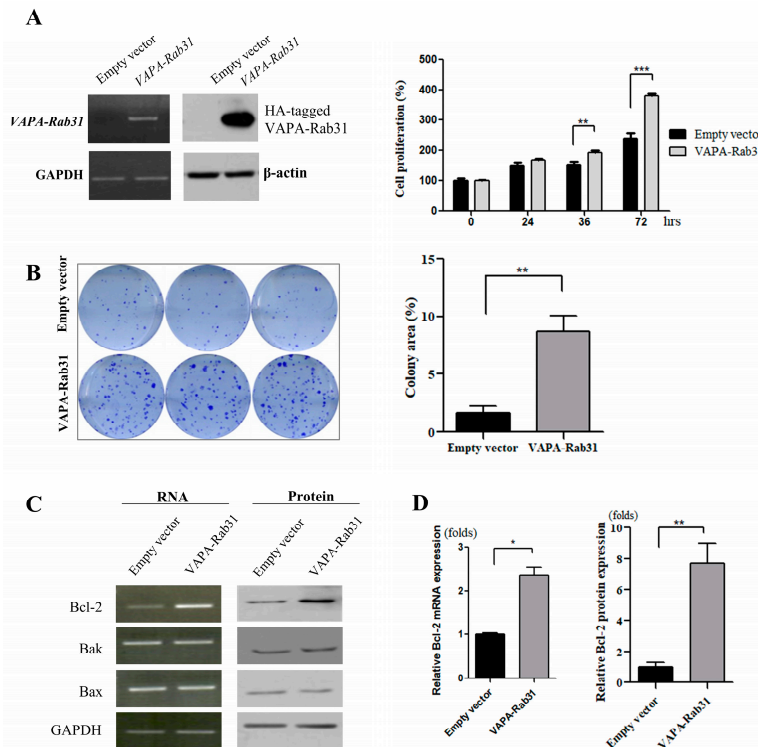


Figure 2. Overexpression of VAPA-Rab31 fusion increases proliferation, colony forming activity, and Bcl-2 expression. (A) Lentivirus-mediated overexpression of VAPA-Rab31 in Beas-2B cells was confirmed by RT-PCR and immunoblot assay detecting HA tag. Glyceraldehyde-3-phosphate dehydrogenase (GAPDH) and β -actin was used as control. Bar graphs indicated the relative cell numbers as the mean

percentage (\pm standard error, SE) at the indicated time; the experiments were performed in triplicates. (** $p < 0.01$, *** $p < 0.005$) (B) *VAPA-Rab31*-overexpressing cells and control cells were cultured to compare colony forming activity as demonstrated as representative data. Bar graphs compare the area of colonies that measured using ImageJ software. Data are expressed as means \pm SE from three independent experiments and a significant result is marked with ** (p value < 0.01). (C) Expression of Bcl-2, Bak and Bax were examined by RT-PCR and Western blotting. (D) The graph indicates the fold change of Bcl-2 expression relative to the expression in control cells. Statistical differences are marked with * ($p < 0.05$), and ** ($p < 0.01$), respectively.

2.3. *VAPA-Rab31* Fusion Induces Resistance to Apoptosis

To examine the effect of *VAPA-Rab31* on apoptosis, the apoptotic markers were compared after induction of apoptosis through bortezomib treatment. Cell cycle analysis revealed that the proportion of sub-G1 phase cells was smaller in the *VAPA-Rab31*-overexpressing cells than in the control cells (Figure 3A). The cleaved PARP and active Caspase-3 were strongly induced in the control cells after bortezomib treatment. However, the cleavage of PARP and the active form of Caspase-3 in *VAPA-Rab31*-overexpressing cells was not induced as much as the control cells after bortezomib treatment indicating reduced apoptosis (Figure 3B). The levels of relevant proteins and their phosphorylation were examined in cytosol, nucleus and whole cells. In *VAPA-Rab31*-expressing cells, Bcl-2 protein and phosphorylated CREB at serine 133 (p-CREB) were retained upregulation even after bortezomib treatment. Phosphorylated Erk (Thr202/Tyr204) was also increased in the nuclear fraction of *VAPA-Rab31*-expressing cells (Figure 3C).

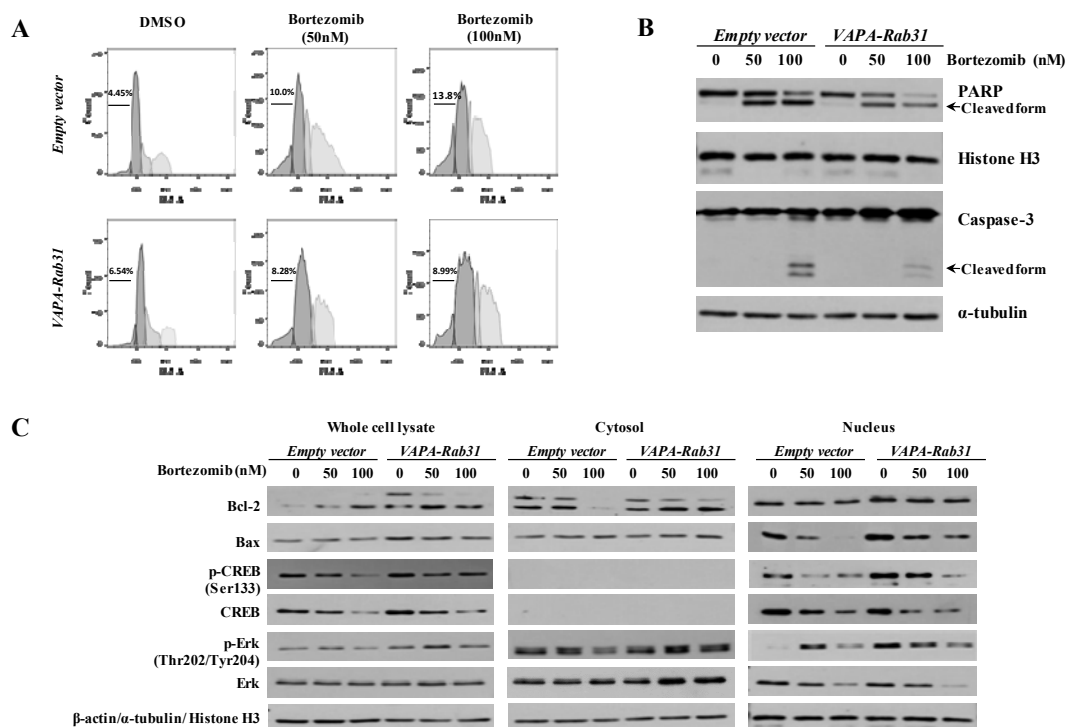


Figure 3. The *VAPA-Rab31* fusion gene induced the resistance to apoptosis. (A) Cell cycle was analyzed in 48 h after bortezomib treatment at the indicated concentration. The percentage of cells in sub-G1 phase (%) was indicated. (B) Cleavage of PARP and Caspase-3 were examined as the apoptotic markers by western blotting at 48 h after bortezomib treatment. (C) Protein expression was examined in whole cell lysates, cytosolic fractions, and nuclear fractions. Phosphorylated CREB and CREB were highly expressed in the nuclear fractions and did not detected in the cytosolic fractions. β -actin, α -tubulin, and histone H3 were used as loading control for whole cell lysates, cytosolic fraction, and nuclear fraction, respectively.

2.4. Tumorigenic Effect of VAPA-Rab31 Fusion is Confirmed Using Xenografts

Furthermore, we examined the effects of *VAPA-Rab31* fusion on tumor growth in vivo using mouse xenograft model in which *VAPA-Rab31*-overexpressing Beas-2B cells were injected subcutaneously. Tumor growth was dramatically increased in mice that were injected with the *VAPA-Rab31*-overexpressing cells (Figure 4A,B). Specifically, control Beas-2B cells did not produce tumors in mice, while *VAPA-Rab31*-overexpressing cells induced subcutaneous tumors in all injected NOG mice as well as the Balb/c nude mice. Furthermore, we found additional tumors in the lungs and liver the *VAPA-Rab31*-xenografted NOG mice. The histologic feature of the tumors was confirmed by hematoxylin and eosin (H&E) staining of formalin-fixed paraffin-embedded (FFPE) tissues that were resected from the mice. Expression of *VAPA-Rab31* protein were confirmed by immunohistochemistry using hemagglutinin (HA) tag antibody. Additionally, we observed high expression of phosphorylated CREB by immunohistochemistry in the primary tumors and lung and liver metastases of NOG mice (Figure 4C).

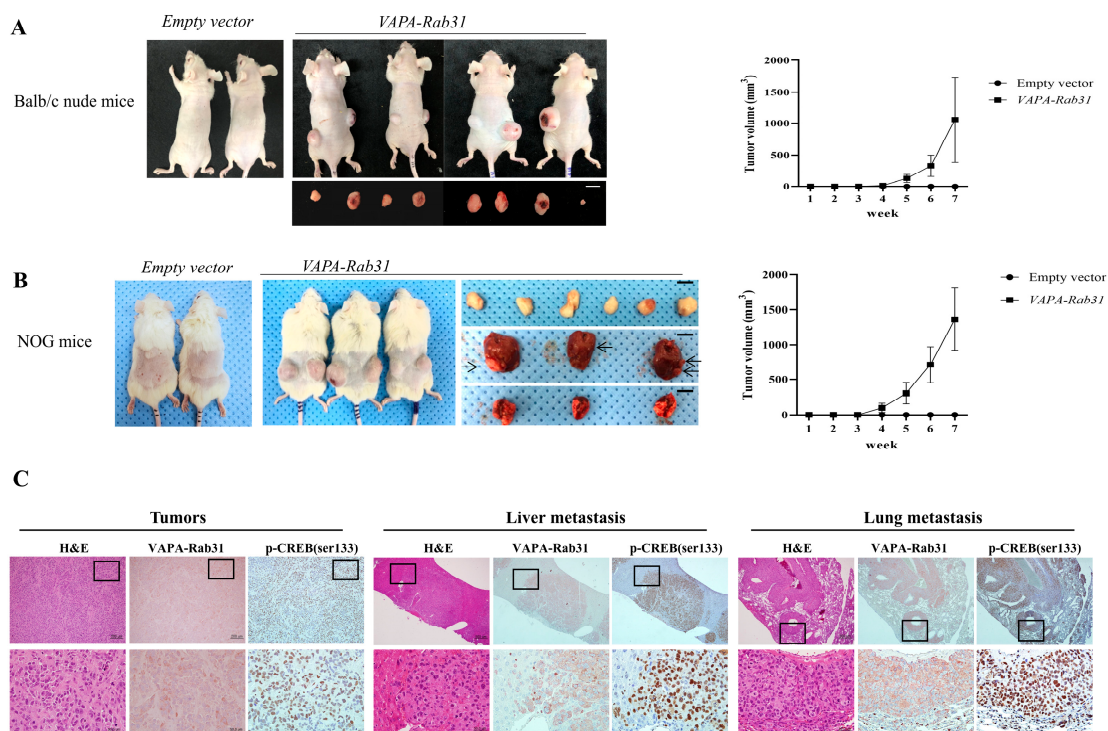


Figure 4. VAPA-Rab31 induces tumorigenesis in the xenograft models. (A,B) *VAPA-Rab31*-overexpressing cells and control cells were injected subcutaneously to Balb/c athymic nude mice (A) and NOG mice (B) to compare tumorigenicity. Growth curve of tumors (■) indicated tumor size at the indicated time. Control cells that overexpressed empty vector (●) did not induce tumors in the xenograft mice. Tumors were resected from mice injected with *VAPA-Rab31*-overexpressing cells. In NOG mice, tumors were observed in lungs and liver, as indicated by arrows. (C) Tumor tissues were examined by H&E staining. Immunohistochemistry demonstrated overexpression of the HA-tagged *VAPA-Rab31* and phosphorylated CREB (p-CREB (ser133)) in tumor cells of subcutaneous tumors, as well as metastatic tumors from liver and lungs.

3. Discussion

Fusion transcripts of *VAPA-Rab31* have been detected in lung adenocarcinoma and hepatocellular carcinoma (TCGA-LIHC/TCGA-ZP-A9D0). However, the tumorigenicity of the *VAPA-Rab31* fusion protein has not yet been investigated. This study demonstrated the oncogenic effect of *VAPA-Rab31* fusion in vivo as well as in vitro. Notably, tumor formation in the xenograft mice injected with *VAPA-Rab31*-overexpressing cells was also associated with metastasis formation in lungs and liver.

The somatic mutations that can drive cancer are promising biomarkers and targets for treatment. Gene fusions can also act as oncogenic drivers, and their characterization has been of great importance to identify additional potential candidates [20–22]. Gene fusion events can occur because of an exogenous carcinogenic environment or endogenous factors such as ionization radiation, oxidative stress, and DNA damage. DNA double-strand breaks are mostly repaired by common molecular mechanisms including non-homologous end-joining that can generate gene fusions in the event of erroneous joining [23,24]. We have to identify the specific gene rearrangements that might favor the development of cancer. Cancer specific expression of fusion genes can be a good condition to select oncogenes. In this regard, RNA sequencing in genome level can detect genetic rearrangements in a broad range of tumor types [25,26]. We observed *VAPA-Rab31* overexpression in the tumor tissue from a patient and not in the paired normal tissue. The expression level of *Rab31* mRNA was similar in tumor and normal tissue. However, cells expressing *VAPA-Rab31* might be selected and expanded during cancer progression because of a growth and/or survival advantage. Beas-2B cells are immortalized epithelial cells isolated from normal human bronchus and cannot induce tumors in immunosuppressed mice [27]. After ectopic expression of *VAPA-Rab31*, Beas-2B cells demonstrated enhanced colony-forming activity and tumorigenicity in a xenograft model.

In this study, we found that *Rab31-VAPA* inhibited apoptosis by increasing the *Bcl-2/Bax* ratio, consistent with the previously identified function of *Rab31* [18]. Overexpression of *VAPA-Rab31* upregulated *Bcl-2* both at the mRNA and protein level and made cells resistant to apoptosis. These results show that *VAPA-Rab31* contributes to oncogenic condition through inhibition of apoptosis, a known cancer hallmark that plays a role in tumor progression [28].

Wilson et al. have previously reported that the cyclic AMP response element (CRE) site in the *Bcl-2* promoter seems to be a major positive regulatory site for *Bcl-2* expression [29]. CRE-binding protein (CREB), a transcription factor for *Bcl-2* expression, is activated by phosphorylation at serine 133 [30,31]. In this study, we found that tumors and metastases that were induced by *VAPA-Rab31* showed strong expression of phosphorylated CREB. Our results therefore suggest that upregulated *Bcl-2* and activated CREB could be a potential mechanism underlying the oncogenic effect of *VAPA-Rab31*. However, further functional analysis is necessary to understand the molecular mechanisms of *VAPA-Rab31*-directed cancer progression.

In conclusion, we suggest that *VAPA-Rab31* might be a novel oncogenic fusion gene that can be occurred upon genetic rearrangement in lung adenocarcinoma.

4. Materials and Methods

4.1. Patient's Specimen and Cell Lines

We investigated the fusion gene *VAPA-Rab31*, discovered from RNA-seq data of a Korean patient with lung adenocarcinoma. RNA-seq data was generated after being approved by the Institutional Review Board (IRB No. NCC-2014-0115) of National Cancer Center Korea (NCCCK). Tumor tissue and adjacent normal tissues of the patient were provided by the tumor bank of NCCCK.

Human bronchial epithelial cells Beas-2 were purchased from American Type Culture Collection (ATCC) and cultured in airway epithelial cell basal medium using a bronchial epithelial cell growth kit (ATCC, Rockville, MD, USA).

4.2. RNA Extraction and RT-PCR

Total RNA was isolated and reverse transcribed into cDNA using the two-step RT-PCR kit (Invitrogen, Carlsbad, CA, USA). To confirm the expression of the *VAPA-Rab31* fusion gene, RT-PCR analysis was performed using primers spanning the breakpoint of the fusion in tumor and adjacent normal tissue of the patient. The fusion junction was amplified using primers spanning the breakpoint (forward primer, 5'-GAACCTAGCAAAGCTGTTCCAC-3' and reverse

primer, 5'-TACATGGGAGCCAATGAATG-3'). The expression of Bcl-2, Bax, and Bak was evaluated by RT-PCR with specific primers. GAPDH was used as quantitative control.

4.3. Overexpression of VAPA-Rab31

The full-length ORF of VAPA-Rab31 was cloned from tumor RNA of the patient, and then inserted into a lentiviral vector with CMV promoter and expressing green fluorescent protein (GFP) as a transduction marker. Lentiviruses of expressing VAPA-Rab31 were generated from HEK293T cells according to the protocol [32]. Briefly, HEK293T cells were transfected with plasmid mixture including expression vector, lentiviral packaging plasmid, psPAX2, and envelope plasmid, pMD2.G using Lipofectamine® 2000 (Invitrogen). After 48 h, the viral supernatants were harvested and filtered. Virus particles were concentrated for the infection. Beas-2B cells were infected with lentiviruses and stably VAPA-Rab31-overexpressing cells were identified because of GFP intensity.

4.4. Proliferation and Colony Formation Assay

Beas-2B cells were seeded in 96-well plates (1.0×10^4 cells/well) to assay their proliferation using the IncuCyte™ Zoom system (Essen BioScience, Michigan, MI, USA) according to the manufacturer's instructions. To test the effect of the VAPA-Rab31 fusion gene on colony formation, cells were seeded in 6-well plates (2.0×10^2 cells/well) and incubated in the appropriate medium, replaced with fresh media every three days. After two weeks, the cells were fixed with 10% methanol and 10% acetic acid and stained with 0.5% crystal violet solution (Sigma-Aldrich, St. Louis, MO, USA). The number of colonies and surface area were measured using the Image J software (National Institutes of Health, Bethesda, MD, USA). Each experiment was performed in triplicates and repeated three times.

4.5. Apoptosis Analysis

A proteasome inhibitor, bortezomib (BioVision Inc., Milpitas, CA, USA) was added to the cells for 48 h to induce apoptosis. Harvested cells were fixed in 70% ethanol and stained with propidium iodide (Sigma-Aldrich). Cell cycle was analyzed by flow cytometry (FACScalibur II, BD Biosciences, MD, USA) and the proportion of cells in sub-G1 phase was determined. The cleaved form of Caspase-3 and PARP were examined as apoptotic markers by western blot analysis.

4.6. Western Blot Analysis

Proteins were extracted in sample buffer (125 mM Tris-HCl, 20% glycerol, 4% sodium dodecyl sulfate (SDS), and 10% 2-mercaptoethanol), quantified, separated by SDS-polyacrylamide gel electrophoresis, and transferred to membranes. Membranes were incubated with specific antibodies and developed using the electrochemiluminescence method (Amersham Life Science, Buckinghamshire, UK). Antibodies for Bcl-2 and Bax were purchased from BD Science (San Jose, CA, USA) while Caspase-3, CREB, phosphorylated CREB were purchased from Santa Cruz Biotechnology (Dallas, TX, USA). Antibodies against PARP, histone H3, Erk, phosphorylated Erk1/2 (Thr202/Tyr204) and horseradish peroxidase-conjugated secondary antibodies were obtained from Cell Signaling Technology (Danvers, MA, USA). Cytosolic and nuclear fractions were prepared using NE-PER Nuclear and Cytoplasmic Extraction kit (ThermoFisher Scientific, GA, USA). Representative data from three independent experiments were demonstrated.

4.7. Induction of In Vivo Tumorigenicity

Six-week-old male Balb/c athymic mice and NOG (NOD.Cg-Prkdcscid II2rgtm1Sug/Jic) mice were purchased from Seron Bio (Kyeonggi, Korea). Beas-2B cells (5.0×10^6 cells/0.1mL PBS) expressing VAPA-Rab31 or the empty vector were injected subcutaneously into the flanks of the mice ($n = 6$ per group). Tumor size and body weight of mice were measured twice a week. Tumor volume was calculated on the indicated days using the following equation: tumor volume = (large

diameter \times smaller diameter²)/2 [33]. Within eight weeks, mice were sacrificed and tumors and organs were harvested for further analysis. Resected tissues were fixed in 4% paraformaldehyde solution and embedded in paraffin. Sections of FFPE tissue were stained with H&E and also analyzed by immunohistochemistry. Briefly, deparaffinized sections were treated with sodium citrate buffer for antigen retrieval, and then incubated with normal serum with 1% bovine serum albumin to block non-specific antibody binding. After incubation with the primary antibodies and biotinylated secondary antibodies, tissues were processed to enzymatic detection with 3,3'-diaminobenzidine substrate. All animal experiments in this study were performed in accordance with the guidelines of the Institutional Animal Care and Use Committee (IACUC) (approval no: KU17167, approved date: 8 November 2017).

4.8. Statistical Analysis

Data were compared to test statistical significance by unpaired *t*-Test using GraphPad Prism software (GraphPad Software Inc., San Diego, CA, USA). All reported *p* values are two-sided and significant differences are marked with * (*p* < 0.05), ** (*p* < 0.01), and *** (*p* < 0.005) on figures, respectively.

Supplementary Materials: Supplementary materials can be found at <http://www.mdpi.com/1422-0067/20/9/2309/s1>.

Author Contributions: Conceptualization, K.-A.Y.; Acquisition of data and methodology, D.Y., K.B. and J.-H.K.; experimental data analysis, K.-A.Y., K.B. and Y.-K.C.; writing and review of the manuscript, K.-A.Y., D.Y., and K.B.; funding acquisition, K.-A.Y. All authors read and approved the final manuscript.

Funding: This work was supported by a grant of the National Research Foundation of Korea (NRF-2017R1E1A1A01073415 to K.-A. Yoon) from the Korean Government.

Acknowledgments: We would like to thank Min Kyoung Lee for technical support.

Conflicts of Interest: The authors declare no conflict of interest.

Abbreviations

VAPA	Vesicle-associated membrane protein (VAMP)-associated protein A
Rab31	Ras-related protein 31
CREB	CAMP responsive element binding protein
PARP	Poly (ADP-ribose) polymerase
Bax	Bcl-2 associated X
Bak	Bcl-2-antagonist/Killer
H&E	Hematoxylin and eosin
FFPE	Formalin-fixed paraffin-embedded

References

1. Bray, F.; Ferlay, J.; Soerjomataram, I.; Siegel, R.L.; Torre, L.A.; Jemal, A. Global cancer statistics 2018: GLOBOCAN estimates of incidence and mortality worldwide for 36 cancers in 185 countries. *CA Cancer J. Clin.* **2018**, *68*, 394–424. [[CrossRef](#)] [[PubMed](#)]
2. Ferlay, J.; Soerjomataram, I.; Dikshit, R.; Eser, S.; Mathers, C.; Rebelo, M.; Parkin, D.M.; Forman, D.; Bray, F. Cancer incidence and mortality worldwide: Sources, methods and major patterns in GLOBOCAN 2012. *Int. J. Cancer* **2015**, *136*, E359–E386. [[CrossRef](#)] [[PubMed](#)]
3. Travis, W.D.; Brambilla, E.; Nicholson, A.G.; Yatabe, Y.; Austin, J.H.M.; Beasley, M.B.; Chirieac, L.R.; Dacic, S.; Duhig, E.; Flieder, D.B.; et al. The 2015 World Health Organization Classification of Lung Tumors: Impact of Genetic, Clinical and Radiologic Advances Since the 2004 Classification. *J. Thorac. Oncol.* **2015**, *10*, 1243–1260. [[CrossRef](#)] [[PubMed](#)]
4. Cheng, L.; Alexander, R.E.; Maclennan, G.T.; Cummings, O.W.; Montironi, R.; Lopez-Beltran, A.; Cramer, H.M.; Davidson, D.D.; Zhang, S. Molecular pathology of lung cancer: Key to personalized medicine. *Mod. Pathol.* **2012**, *25*, 347–369. [[CrossRef](#)] [[PubMed](#)]
5. The Cancer Genome Atlas Research Network. Comprehensive molecular profiling of lung adenocarcinoma. *Nature* **2014**, *511*, 543–550. [[CrossRef](#)]

6. Jordan, E.J.; Kim, H.R.; Arcila, M.E.; Barron, D.; Chakravarty, D.; Gao, J.; Chang, M.T.; Ni, A.; Kundra, R.; Jonsson, P.; et al. Prospective Comprehensive Molecular Characterization of Lung Adenocarcinomas for Efficient Patient Matching to Approved and Emerging Therapies. *Cancer Discov.* **2017**, *7*, 596–609. [[CrossRef](#)]
7. Soda, M.; Choi, Y.L.; Enomoto, M.; Takada, S.; Yamashita, Y.; Ishikawa, S.; Fujiwara, S.; Watanabe, H.; Kurashina, K.; Hatanaka, H.; et al. Identification of the transforming *EML4-ALK* fusion gene in non-small-cell lung cancer. *Nature* **2007**, *448*, 561–566. [[CrossRef](#)]
8. Pan, Y.; Zhang, Y.; Li, Y.; Hu, H.; Wang, L.; Li, H.; Wang, R.; Ye, T.; Luo, X.; Zhang, Y.; et al. *ALK*, *ROS1* and *RET* fusions in 1139 lung adenocarcinomas: A comprehensive study of common and fusion pattern-specific clinicopathologic, histologic and cytologic features. *Lung Cancer* **2014**, *84*, 121–126. [[CrossRef](#)] [[PubMed](#)]
9. Stransky, N.; Cerami, E.; Schalm, S.; Kim, J.L.; Lengauer, C. The landscape of kinase fusions in cancer. *Nat. Commun.* **2014**, *5*, 4846. [[CrossRef](#)] [[PubMed](#)]
10. Campbell, J.D.; Alexandrov, A.; Kim, J.; Wala, J.; Berger, A.H.; Peadarallu, C.S.; Shukla, S.A.; Guo, G.; Brooks, A.N.; Murray, B.A.; et al. Distinct patterns of somatic genome alterations in lung adenocarcinomas and squamous cell carcinomas. *Nat. Genet.* **2016**, *48*, 607–616. [[CrossRef](#)] [[PubMed](#)]
11. Shaw, A.T.; Ou, S.H.; Bang, Y.J.; Camidge, D.R.; Solomon, B.J.; Salgia, R.; Riely, G.J.; Varella-Garcia, M.; Shapiro, G.I.; Costa, D.B.; et al. Crizotinib in *ROS1*-rearranged non-small-cell lung cancer. *N. Engl. J. Med.* **2014**, *371*, 1963–1971. [[CrossRef](#)]
12. Solomon, B.J.; Mok, T.; Kim, D.W.; Wu, Y.L.; Nakagawa, K.; Mekhail, T.; Felip, E.; Cappuzzo, F.; Paolini, J.; Usari, T.; et al. First-line crizotinib versus chemotherapy in *ALK*-positive lung cancer. *N. Engl. J. Med.* **2014**, *371*, 2167–2177. [[CrossRef](#)]
13. Kelly, E.E.; Horgan, C.P.; Goud, B.; McCaffrey, M.W. The Rab family of proteins: 25 years on. *Biochem. Soc. Trans.* **2012**, *40*, 1337–1347. [[CrossRef](#)]
14. Chua, C.E.; Tang, B.L. Engagement of the small GTPase Rab31 protein and its effector, early endosome antigen 1, is important for trafficking of the ligand-bound epidermal growth factor receptor from the early to the late endosome. *J. Biol. Chem.* **2014**, *289*, 12375–12389. [[CrossRef](#)]
15. Chua, C.E.; Tang, B.L. The role of the small GTPase Rab31 in cancer. *J. Cell. Mol. Med.* **2015**, *19*, 1–10. [[CrossRef](#)]
16. Pan, Y.; Zhang, Y.; Chen, L.; Liu, Y.; Feng, Y.; Yan, J. The Critical Role of Rab31 in Cell Proliferation and Apoptosis in Cancer Progression. *Mol. Neurobiol.* **2016**, *53*, 4431–4437. [[CrossRef](#)]
17. Grismayer, B.; Solch, S.; Seubert, B.; Kirchner, T.; Schafer, S.; Baretton, G.; Schmitt, M.; Luther, T.; Kruger, A.; Kotsch, M.; et al. Rab31 expression levels modulate tumor-relevant characteristics of breast cancer cells. *Mol. Cancer* **2012**, *11*, 62. [[CrossRef](#)]
18. Sui, Y.; Zheng, X.; Zhao, D. Rab31 promoted hepatocellular carcinoma (HCC) progression via inhibition of cell apoptosis induced by PI3K/AKT/Bcl-2/BAX pathway. *Tumour Biol.* **2015**, *36*, 8661–8670. [[CrossRef](#)]
19. Nishimura, Y.; Hayashi, M.; Inada, H.; Tanaka, T. Molecular cloning and characterization of mammalian homologues of vesicle-associated membrane protein-associated (VAMP-associated) proteins. *Biochem. Biophys. Res. Commun.* **1999**, *254*, 21–26. [[CrossRef](#)]
20. Shaw, A.T.; Hsu, P.P.; Awad, M.M.; Engelman, J.A. Tyrosine kinase gene rearrangements in epithelial malignancies. *Nat. Rev. Cancer* **2013**, *13*, 772–787. [[CrossRef](#)] [[PubMed](#)]
21. Mertens, F.; Johansson, B.; Fioretos, T.; Mitelman, F. The emerging complexity of gene fusions in cancer. *Nat. Rev. Cancer* **2015**, *15*, 371–381. [[CrossRef](#)]
22. Yoshihara, K.; Wang, Q.; Torres-Garcia, W.; Zheng, S.; Vegesna, R.; Kim, H.; Verhaak, R.G. The landscape and therapeutic relevance of cancer-associated transcript fusions. *Oncogene* **2015**, *34*, 4845–4854. [[CrossRef](#)]
23. Mani, R.S.; Chinnaiyan, A.M. Triggers for genomic rearrangements: Insights into genomic, cellular and environmental influences. *Nat. Rev. Genet.* **2010**, *11*, 819–829. [[CrossRef](#)]
24. Mani, R.S.; Tomlins, S.A.; Callahan, K.; Ghosh, A.; Nyati, M.K.; Varambally, S.; Palanisamy, N.; Chinnaiyan, A.M. Induced chromosomal proximity and gene fusions in prostate cancer. *Science* **2009**, *326*, 1230. [[CrossRef](#)] [[PubMed](#)]
25. Maher, C.A.; Kumar-Sinha, C.; Cao, X.; Kalyana-Sundaram, S.; Han, B.; Jing, X.; Sam, L.; Barrette, T.; Palanisamy, N.; Chinnaiyan, A.M. Transcriptome sequencing to detect gene fusions in cancer. *Nature* **2009**, *458*, 97–101. [[CrossRef](#)] [[PubMed](#)]

26. Maher, C.A.; Palanisamy, N.; Brenner, J.C.; Cao, X.; Kalyana-Sundaram, S.; Luo, S.; Khrebtukova, I.; Barrette, T.R.; Grasso, C.; Yu, J.; et al. Chimeric transcript discovery by paired-end transcriptome sequencing. *Proc. Natl. Acad. Sci. USA* **2009**, *106*, 12353–12358. [[CrossRef](#)]
27. Albright, C.D.; Jones, R.T.; Hudson, E.A.; Fontana, J.A.; Trump, B.F.; Resau, J.H. Transformed human bronchial epithelial cells (BEAS-2B) alter the growth and morphology of normal human bronchial epithelial cells in vitro. *Cell Biol. Toxicol.* **1990**, *6*, 379–398. [[CrossRef](#)]
28. Hanahan, D.; Weinberg, R.A. Hallmarks of cancer: The next generation. *Cell* **2011**, *144*, 646–674. [[CrossRef](#)]
29. Wilson, B.E.; Mochon, E.; Boxer, L.M. Induction of bcl-2 expression by phosphorylated CREB proteins during B-cell activation and rescue from apoptosis. *Mol. Cell. Biol.* **1996**, *16*, 5546–5556. [[CrossRef](#)]
30. Naqvi, S.; Martin, K.J.; Arthur, J.S. CREB phosphorylation at Ser133 regulates transcription via distinct mechanisms downstream of cAMP and MAPK signalling. *Biochem. J.* **2014**, *458*, 469–479. [[CrossRef](#)]
31. Sakamoto, K.M.; Frank, D.A. CREB in the pathophysiology of cancer: Implications for targeting transcription factors for cancer therapy. *Clin. Cancer Res.* **2009**, *15*, 2583–2587. [[CrossRef](#)] [[PubMed](#)]
32. Tiscornia, G.; Singer, O.; Verma, I.M. Production and purification of lentiviral vectors. *Nat. Protoc.* **2006**, *1*, 241–245. [[CrossRef](#)] [[PubMed](#)]
33. Lee, J.Y.; Kim, M.S.; Kim, E.H.; Chung, N.; Jeong, Y.K. Retrospective growth kinetics and radiosensitivity analysis of various human xenograft models. *Lab. Anim. Res.* **2016**, *32*, 187–193. [[CrossRef](#)] [[PubMed](#)]



© 2019 by the authors. Licensee MDPI, Basel, Switzerland. This article is an open access article distributed under the terms and conditions of the Creative Commons Attribution (CC BY) license (<http://creativecommons.org/licenses/by/4.0/>).